

# Semiclassical propagator approach for emission processes.

## I. Two-body non-relativistic case

S.A. Ghinescu<sup>1,2\*</sup> and D.S. Delion<sup>1,2,3,4</sup>

<sup>1</sup> "Horia Hulubei" National Institute of Physics and Nuclear Engineering,  
30 Reactorului, POB MG-6, RO-077125, Bucharest-Măgurele, România

<sup>2</sup> Department of Physics, University of Bucharest, 405 Atomîștilor,  
POB MG-11, RO-077125, Bucharest-Măgurele, România

<sup>3</sup> Academy of Romanian Scientists, 3 Ilfov RO-050044, Bucharest, România

<sup>4</sup> Bioterra University, 81 Gârlei RO-013724, Bucharest, România

(Dated: February 17, 2021)

We compare the coupled channels procedure to the semiclassical approach to describe two-body emission processes, in particular  $\alpha$ -decay, from deformed nuclei within the propagator method. We express the scattering amplitudes in terms of a propagator matrix, describing the effect of the deformed field, multiplied by the ratio between internal wave function components and irregular Coulomb waves. In the spherical case the propagator becomes diagonal and scattering amplitudes acquire the well-known form. We describe a more rigorous formulation of the 3D semiclassical approach, corresponding to deformed potentials, which leads to the exact results and we also compare them with the much simpler expressions given by the Angular Wentzel-Kramers-Brillouin (AWKB) and Linearized WKB (LWKB) with its approximation, known as Fröman WKB (FWKB) method. We will show that LWKB approach is closer than AWKB to the exact coupled-channels formalism. An analysis of alpha-emission from ground states of even-even nuclei evidences the important role played by deformation upon the channel decay widths.

### I. INTRODUCTION

The exact description of emission processes is provided by outgoing solutions in continuum of the equation of motion. When the masses of the emitted particles are much larger than the energy release (Q-value) the non-relativistic Schrödinger equation is used, while in the other case a relativistic approach is employed within the Klein-Gordon equation for boson emission and Dirac equation for fermion emission. The case of non-relativistic two-body processes refers by the one proton emission, alpha and heavy cluster decays  $P \rightarrow D + C$ , while two-proton emission  $P \rightarrow D + p + p$  belongs to the field of non-relativistic three-body dynamics. The most important relativistic three-body emission processes is given by the  $\beta^+$  decay  $p \rightarrow n + e^+ + \nu$ , where the positron mass has a comparable value to the Q-value but it penetrates a very large barrier, comparable to the proton emission case. The exact solutions for deformed emitters in all these cases are provided within the coupled channels (CC) approach with an outgoing asymptotics [1]. All these processes are basically described by the quantum penetration of a particle/cluster through an internal nuclear plus an external Coulomb barrier, characterized by a relative small ratio between the Q-value and barrier height. In this case semiclassical solutions provide very good approximations and our purpose is to analyze such solutions in the most general cases, by applying the so-called propagator method, already described for the CC approach in Ref. [1].

We will describe in this paper the two-body non-relativistic emission, where a very good approximation is given by the semiclassical Wentzel-Kramers-Brillouin (WKB) approach [2–4]. The problem of a formulating a general three-dimensional (3D) WKB theory for systems lacking spherical symmetry has a long history. The first successful attempt is due to Fröman [6] who obtained a "semi-analytic" expression for the wave-function of an alpha particle inside a large barrier using geometrical considerations. His attempt is not, however, free from caveats especially due to the *intuitive* approach he followed. We present here a more rigorous formulation which leads to the so called Linearized WKB (LWKB), which has as a particular case the Fröman method. We also compare them with the much simpler expression which has seen extensive use by many authors [4, 5]. We will refer to this method as "Angular WKB" or AWKB, in short. In the end we show that both methods agree with the exact coupled-channels formalism for small to reasonable deformations. We will apply these considerations in the case of alpha decays to ground and excited states.

### II. MATHEMATICAL FORMULATION

To give a full account of all steps we begin with the spherically symmetric problem, the reason being that the centrifugal term in the potential appears naturally when one builds up the deformed solution as an extension of the spherical one.

---

\* Corresponding author: stefan.ghinescu@nipne.ro

### A. Spherical emitters

Let us consider a binary emission process

$$P(J_i) \rightarrow D(J_f) + C(L) \quad (2.1)$$

where  $J_{i/f}$  denotes the initial/final spin<sup>parity</sup> of the parent (P)/daughter (D) nucleus and  $L$  the angular momentum carried by the emitted cluster (C). For simplicity we consider the cluster with a boson structure (an alpha particle or heavier cluster). We will also assume an initial ground state  $J_i = 0$ , leading to  $J_f = L$ , i.e. a coupled daughter-cluster dynamics with the total spin  $L \otimes L = 0$ . The Schrödinger equation governs the dynamics of the binary D+C system inside a spherically symmetric potential barrier  $V_0(r)$

$$\left[ -\frac{\hbar^2}{2\mu} \Delta + V_0(r) \right] \Psi_0(\mathbf{r}) = E \Psi_0(\mathbf{r}) , \quad (2.2)$$

where  $\mathbf{r} = (r, \theta, \phi)$  denotes the position vector of the cluster in the center of mass (CM) of the system in spherical coordinates and  $\mu = m_C m_D / (m_C + m_D)$  defines the daughter-cluster reduced mass. The generalisation to the emission of fermions is straightforward. Notice that inside the external Coulomb barrier the standard multipole expansion

$$\Psi_0(\mathbf{r}) = \sum_L \frac{f_L(r)}{r} Y_{L0}(\theta) , \quad (2.3)$$

leads at a large distance to the following equations for radial components

$$\left[ -\frac{d^2}{d\rho^2} + \frac{L(L+1)}{\rho^2} + \frac{\chi}{\rho} - 1 \right] f_l(r) = 0 , \quad (2.4)$$

depending upon the Coulomb parameter

$$\chi = \frac{2Z_D Z_C}{\hbar v} , \quad (2.5)$$

and reduced radius

$$\rho = kr, \quad k = \sqrt{\frac{2\mu E}{\hbar^2}} . \quad (2.6)$$

We employ the semiclassical ansatz by writing

$$\Psi_0(\mathbf{r}) \equiv \exp \left[ \frac{i}{\hbar} S_0(\mathbf{r}) \right] . \quad (2.7)$$

Upon inserting this expression in Eq. (2.2), we obtain

$$-\frac{i\hbar}{2\mu} \Delta S_0(\mathbf{r}) + \frac{1}{2\mu} [\nabla S_0(\mathbf{r})]^2 + V_0(r) = E , \quad (2.8)$$

where  $\Delta$  and  $\nabla$  denote the laplacian and gradient respectively in spherical coordinates.

The semiclassical prescription requires the exponent  $S_0(\mathbf{r})$  to be expanded in powers of  $\hbar$  as  $S_0(\mathbf{r}) = S_0^{(0)}(\mathbf{r}) + \hbar S_0^{(1)}(\mathbf{r})$ . We plug the expansion in Eq. (2.8) and group

coefficients of equal powers of  $\hbar$  to obtain the following system of equations

$$\begin{aligned} \hbar^0 : \left( \nabla S_0^{(0)}(\mathbf{r}) \right)^2 &= -K_0^2(r) \\ \hbar^1 : -\frac{i}{2} \Delta S_0^{(0)}(\mathbf{r}) + (\nabla S_0^{(0)}(\mathbf{r}))(\nabla S_0^{(1)}(\mathbf{r})) &= 0 , \end{aligned} \quad (2.9)$$

where we defined the "radial dependent momentum"

$$K_0(r) \equiv \sqrt{2\mu E \left[ \frac{V_0(r)}{E} - 1 \right]} . \quad (2.10)$$

We show in the Appendix that an "outgoing" solution of this system is given by

$$\Psi_0(r, \theta) = \sum_L \frac{c_L Y_{L0}^{(WKB)}(\theta)}{\sqrt{K_{0,L}(r)}} \exp \left[ \int_r^{r_2} dr K_{0,L}(r) \right] , \quad (2.11)$$

where  $Y_{L0}^{(WKB)}$  is the spherical harmonic  $Y_{L0}$  in the WKB approximation,  $c_L$  are some constants,  $r_2$  is the external turning point defined as the largest solution of the equation  $V_0(r_2) = E$  and

$$K_{0,L}(r) \equiv \sqrt{2\mu E \left[ \frac{V_0(r)}{E} - 1 + \frac{(L + \frac{1}{2})^2}{k^2 r^2} \right]} . \quad (2.12)$$

Note that we have dropped the  $\phi$  dependence, which appears only in the form of a phase since the potential is spherically symmetric. This simplifies expressions in both the spherical and deformed cases without loss of generality.

### B. Deformed emitters

We turn now to solving the deformed problem. In the laboratory system of coordinates the dynamics of the emission process (2.1) is described by the following Schrödinger equation

$$\left[ \hat{\mathbf{H}}(\mathbf{R}) + \hat{\mathbf{H}}_D(\Omega) + V(\mathbf{R}, \Omega) \right] \Phi(\mathbf{R}, \Omega) = E \Phi(\mathbf{R}, \Omega) , \quad (2.13)$$

where  $\hat{\mathbf{H}}(\mathbf{R})$  denotes the Hamiltonian of the daughter-cluster motion depending on the relative coordinate  $\mathbf{R} = (r, \hat{R})$  and  $\hat{\mathbf{H}}_D(\Omega)$  describes the internal daughter motion depending on its coordinate  $\Omega$ , which is given by Euler angles for rotational motion. We will consider an axially symmetric daughter-cluster interaction which can be estimated within the double folding procedure [7–9] by the following expansion

$$\begin{aligned} V(\mathbf{R}, \Omega) &= V_0(r) + \sum_{\lambda > 0} V_\lambda(r) \sqrt{\frac{4\pi}{2\lambda + 1}} \left[ Y_\lambda(\Omega) \otimes Y_\lambda(\hat{R}) \right]_0 \\ &= V_0(r) + \sum_{\lambda > 0} V_\lambda(r) Y_{\lambda 0}(\hat{r}) \\ &\equiv V_0(r) + V_d(\mathbf{r}) , \end{aligned} \quad (2.14)$$

where  $\hat{r}$  is the daughter-particle angle, defining the intrinsic system of coordinates  $\mathbf{r} = (r, \hat{r})$ , with  $V_0$ , the isotropic component (monopole), and  $V_d(\mathbf{r})$ , the purely anisotropic part. We expand solution in the intrinsic system to obtain in a standard way the coupled system of equations. By neglecting the off-diagonal Coriolis terms within the so-called adiabatic approach one obtains at large distances a similar to (2.4) form, but with different Coulomb parameters and reduced radii in each channel [1, 6]

$$\begin{aligned} \chi_L &= \frac{\chi}{\epsilon_L} \\ \rho_L &= \rho \epsilon_L \\ \epsilon_L &\equiv \sqrt{1 - \frac{E_L}{E}}, \end{aligned} \quad (2.15)$$

where  $E_L$  denotes the excitation energy of the daughter nucleus. This corresponds to the energy replacements  $E \rightarrow E - E_L$  in each channel.

In order to analyze the specific features of the deformed WKB approach we will first neglect the excitations energies of the daughter nucleus, which will be considered later in applications. The corresponding Schrodinger equation now reads

$$\left[ -\frac{\hbar^2}{2\mu} \Delta + V_0(r) + V_d(\mathbf{r}) \right] \Psi(\mathbf{r}) = E \Psi(\mathbf{r}). \quad (2.16)$$

We propose a semiclassical ansatz similar to the one in the spherical case

$$\Psi(\mathbf{r}) = \exp \left[ \frac{i}{\hbar} S(\mathbf{r}) \right], \quad (2.17)$$

from which we obtain the deformed equivalent of the system in Eq. (2.9) by making again the expansion in powers of  $\hbar$  as  $S(\mathbf{r}) = S^{(0)}(\mathbf{r}) + \hbar S^{(1)}(\mathbf{r})$

$$\begin{aligned} \hbar^0 : (\nabla S^{(0)}(\mathbf{r}))^2 &= -K^2(\mathbf{r}) \\ \hbar^1 : -\frac{i}{2} \Delta S^{(0)}(\mathbf{r}) + (\nabla S^{(0)}(\mathbf{r}))(\nabla S^{(1)}(\mathbf{r})) &= 0, \end{aligned} \quad (2.18)$$

where we have defined

$$K(\mathbf{r}) \equiv \sqrt{2\mu E \left[ \frac{V_0(r)}{E} - 1 + \frac{V_d(\mathbf{r})}{E} \right]}. \quad (2.19)$$

The approach followed by Fröman to solve Eqs. (2.18) is known today as the *linearization* of the Eikonal equation which applies to  $S^{(0)}$  in our case. This approximation consists in isolating the spherical part  $K_0(r)$  defined by Eq. (2.10) in the first equation (2.18). We call this approach as Linearized WKB (LWKB). This can be achieved through the binomial approximation if  $V_d$  is small compared with  $V_0$  (in the following we omit the

spatial variables trusting no ambiguity arises)

$$\begin{aligned} K(\mathbf{r}) &= \sqrt{2\mu E \left( \frac{V_0}{E} - 1 \right)} \sqrt{1 + \frac{V_d/E}{V_0/E - 1}} \\ &\approx \sqrt{2\mu E \left( \frac{V_0}{E} - 1 \right)} \left( 1 + \frac{1}{2} \frac{V_d/E}{V_0/E - 1} \right) \\ &\equiv K_0 + \frac{\Delta K}{K_0}, \end{aligned} \quad (2.20)$$

where we have defined

$$\Delta K \equiv \frac{1}{2} 2\mu V_d. \quad (2.21)$$

As we mentioned, Fröman WKB approach (FWKB) is a particular case of LWKB and it corresponds to a pure Coulomb potential of a deformed nucleus with a sharp density distribution. In this case various multipoles of  $V_d$  have closed analytic expressions.

It is clear now that, since we have isolated the spherical contribution, we can use the solution from its associated problem. We write  $S^{(0)}(\mathbf{r})$  as

$$S^{(0)}(\mathbf{r}) = S_0^{(0)}(\mathbf{r}) + D(\mathbf{r}), \quad (2.22)$$

where  $S_0^{(0)}$  is the solution of the spherical problem given by Eq. (2.11), and  $D(\mathbf{r})$  is the correction arising from the potential deformation. Then we replace this definition together with Eqs. (2.20,2.21) inside Eq. (2.18) and obtain

$$\begin{aligned} (\nabla S_0^{(0)})^2 + (\nabla D)^2 + 2(\nabla S_0^{(0)})(\nabla D) &= \\ - \left( K_0^2 + \frac{\Delta K^2}{K_0^2} + 2\Delta K \right). \end{aligned} \quad (2.23)$$

The essence of the linearized eikonal approximation consists in neglecting terms of powers higher than 1 in both  $\Delta K$  and  $\nabla D$ . We enforce now this idea and, after small simplifications, we obtain

$$(\nabla S_0^{(0)})(\nabla D) = -\Delta K. \quad (2.24)$$

As shown in Appendix, the partial derivatives of  $S_0^{(0)}$  are given by

$$\begin{aligned} \frac{\partial S_0^{(0)}}{\partial \theta} &= \left( L + \frac{1}{2} \right) \hbar \\ \frac{\partial S_0^{(0)}}{\partial r} &= \pm i K_{0,L}(r), \end{aligned} \quad (2.25)$$

where  $L$  is the angular momentum quantum number.

We see now that our problem reduces to solving the equation

$$i K_{0,L}(r) \frac{\partial D}{\partial r} + \frac{(L + \frac{1}{2}) \hbar}{r^2} \frac{\partial D}{\partial \theta} = -\Delta K. \quad (2.26)$$

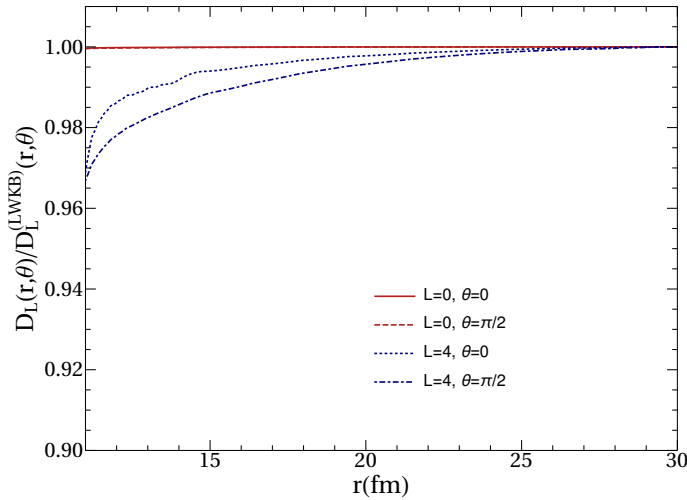


FIG. 1. Ratio between the solution of eq. (2.26) and LWKB approximation versus radius for  $L = 0, 4$  and  $\theta = 0, \pi/2$ .

This equation does not have a closed form solution unless the deformed potential is of the form  $V_d(r, \theta) = \mathcal{V}(\theta)/r^2$ , which is not the case for axial deformations. Consequently, the approximation used is that even though the potential is no longer spherically symmetric, the classical trajectory of the emitted cluster would still be a straight line and one can integrate this system radially by setting formally  $\partial D/\partial\theta = 0$ . This approximation is somewhat justified also by the coefficients of the two partial derivatives: far away from the turning points  $K_{0,L}(r)$  is of the order 1, while  $(L + 1/2)/r \propto 0.1$ . Indeed, we solved numerically equation Eq. (2.26) and plotted the ratio between exact and LWKB solutions in Fig. 1. One notices that the deviation with respect to the LWKB solution is very small.

In this case, the Fröman correction on each channel can be integrated starting from far away from the nucleus, say from a point  $r = r_0$ , where the field is spherical (hence  $D = 0$  for all  $l$ ) and the exponent becomes

$$\frac{i}{\hbar}D(r, \theta) = -\frac{1}{\hbar} \int_{r_0}^r dr' \frac{\Delta K(r', \theta)}{K_{0,L}(r')} . \quad (2.27)$$

We note here that this is the correct use of the WKB approximation since it gives the expected asymptotic behavior, while in [6] the author performs the integration starting from the nuclear surface towards the turning point. This observation is useful, however, only if one desires to compute the wave-function of the alpha particle inside the barrier at a specific point. By contrast, if we wish to compute only the penetrability, both expressions are equally valid.

The last step would be to consider the effect of the deformation on the quantum term  $S^{(1)}$  in Eq. (2.18), but this proves to be quite small compared to what we have discussed already so we omit the correction, keeping only the spherical part  $S^{(1)}(\mathbf{r}) \approx S_0^{(1)}(\mathbf{r})$ . The procedure is the

same, the derivative with respect to  $\theta$  is neglected in the  $S_1$  term and the integration is carried out radially. This approximation performs rather well as we will show in the following section.

We turn our focus on the AWKB method. In the first few paragraphs of this chapter we claimed it is more elegant than the one of Fröman and now we will provide some arguments. In order not to repeat all the equations we refer the reader to the system from Eq. (2.18). If we do not attempt to linearize this equation, the only way towards a "semi-analytic" expression is again radial integration. We set  $\partial S^{(0)}/\partial\theta = 0$ , but this is not enough. We do not retrieve in this way the angular momenta enumeration, hence we still have to separate the spherical contribution. We can do this by writing

$$K^2(\mathbf{r}) = K_0^2(r) + \Delta K^{(\text{AWKB})}(\mathbf{r}) , \quad (2.28)$$

where we have defined

$$\Delta K^{(\text{AWKB})}(\mathbf{r}) = 2\mu V_d(\mathbf{r}) . \quad (2.29)$$

We now use the definition of  $S^{(0)}$  from Eq. (2.22) without neglecting any term to write

$$(\nabla S_0^{(0)})^2 + (\nabla D)^2 + 2(\nabla S_0^{(0)})(\nabla D) = -K_0^2 - \Delta K^{(\text{AWKB})} . \quad (2.30)$$

As per Eq. (2.9),  $(\nabla S_0^{(0)})^2 = -K_0^2$ , and if we set  $\partial D/\partial\theta = 0$  again, we obtain

$$\left(\frac{\partial D}{\partial r}\right)^2 + 2\frac{\partial S_0^{(0)}}{dr} \frac{\partial D}{\partial r} = -\Delta K^{(\text{AWKB})} . \quad (2.31)$$

The derivative of  $S_0^{(0)}$  with respect to  $r$  is given in Eq. (2.25) and we solve this quadratic equation for  $dD/dr$  as

$$\begin{aligned} \frac{\partial D}{\partial r} &= \mp iK_{0,L} \pm i\sqrt{K_{0,L} + \Delta K^{(\text{AWKB})}} \\ &\equiv \mp iK_{0,L}(r) \pm iK_L(\mathbf{r}) , \end{aligned} \quad (2.32)$$

where we have denoted

$$K_L(\mathbf{r}) = \sqrt{2\mu E \left( \frac{V_0}{E} - 1 + \frac{(L + \frac{1}{2})^2}{k^2 r^2} + \frac{V_d(\mathbf{r})}{E} \right)} . \quad (2.33)$$

Upon integrating the last equation, we retrieve the well-known (but not proved) inclusion of the centrifugal potential in the 3D WKB exponent

$$\frac{i}{\hbar}D(r, \theta) = -\frac{i}{\hbar}S_0^{(0)}(r) + \frac{1}{\hbar} \int_r^{r_0} dr' K_L(r', \theta) , \quad (2.34)$$

for some radius  $r_0 > r$  where the function is known. So it turns out that the "mixed" representation where the centrifugal term is included a priori is actually less approximate than Fröman's method, at least in principle. Now, regarding the second term in the expansion, in this case it is given as an extension of the spherical case

$$S^{(1)}(r, \theta) = \frac{i}{2} \ln \sqrt{K_L(r, \theta)} . \quad (2.35)$$

This result follows if one integrates radially the original system of equations with the centrifugal potential inserted in the exponent as described above.

### C. Propagator method

Now, since we have build the wave-functions at all coordinates  $(r, \theta)$ , we can compare the WKB results with the exact coupled channels (CC) one. To achieve this we must build the fundamental matrix of solutions in the WKB case. The exact CC fundamental matrix of solutions is defined by the following asymptotics [1]

$$\mathcal{H}_{LL'}^{(CC)}(r) \rightarrow_{r \rightarrow \infty} H_L^{(+)}(kr, \chi) \delta_{LL'} , \quad (2.36)$$

in terms of the outgoing Coulomb-Hankel spherical waves  $H_L^{(+)}(\chi, kr) = G_L(\chi, kr) + iF_L(\chi, kr)$ . Thus, each column of the fundamental matrix of solutions is obtained by integrating backwards the coupled system of differential equations, starting with above mentioned asymptotic value. Notice that inside the Coulomb barrier this matrix has practically real values, due to the fact that here one has  $G_L(\chi, kr) \gg F_L(\chi, kr)$ . Therefore in practical calculations one uses only the irregular Coulomb wave at large distance. The general solution with a given angular momentum is built as a superposition of columns

$$\begin{aligned} f_L(r) &= \sum_{L'} \mathcal{H}_{LL'}^{(CC)}(r) N_{L'} \\ &\rightarrow_{r \rightarrow \infty} N_L H_L^{(+)}(kr, \chi) . \end{aligned} \quad (2.37)$$

This expression can be used to find scattering amplitudes  $N_L$  in terms of components of the internal function at some radius  $r$  inside the barrier by using the matching condition  $f_L^{(int)}(r) = f_L(r)$

$$N_L = \frac{1}{H_L^{(+)}} \sum_{L'} \mathcal{K}_{LL'}^{(CC)}(r) f_{L'}^{(int)}(r) , \quad (2.38)$$

where we introduced the propagator matrix [1] as follows

$$\begin{aligned} \mathcal{K}_{LL'}^{(CC)}(r) &\equiv H_L^{(+)}(\chi, kr) \left[ \mathcal{H}_{LL'}^{(CC)}(r) \right]^{-1} \\ &\approx G_L(\chi, kr) \left[ \mathcal{H}_{LL'}^{(CC)}(r) \right]^{-1} , \end{aligned} \quad (2.39)$$

with the following property

$$\mathcal{K}_{LL'}^{(CC)}(r) \rightarrow_{V_d \rightarrow 0} \delta_{LL'} , \quad (2.40)$$

which takes place for a spherical interaction, or for a deformed interaction at large distance where it becomes spherical.

We observe from Eqs. (2.27) and (2.34) that the complete wave-function in both cases can be written as

$$\Psi(r, \theta) = \sum_L \psi_L(r, \theta) Y_L(\theta) , \quad (2.41)$$

where  $\psi_L(r, \theta)$  are built up using the WKB functions

$$\psi_L(r, \theta) = \exp \left\{ \frac{i}{\hbar} \left( S^{(0)}(r, \theta) + \hbar S^{(1)}(r, \theta) \right) \right\} , \quad (2.42)$$

with both  $S^{(0)}$  and  $S^{(1)}$  depending on  $L$ , as we have shown. Then, the radial components of the complete wave-function are given by

$$\Psi_L(r) = \sum_{L'} \int d\Omega Y_L \psi_{L'}(r) Y_{L'} , \quad (2.43)$$

which can readily be translated to the fundamental matrix with the asymptotics (2.36) as

$$\mathcal{H}(r) \equiv \mathcal{H}_{L,L'}(r) = \int d\Omega Y_L \psi_{L'}(r) Y_{L'} . \quad (2.44)$$

We now particularize Eq. (2.44) in the AWKB and LWKB approaches. For the AWKB approximation, we have

$$\begin{aligned} \mathcal{H}_{L,L'}^{(AWKB)}(r) &= \int d\Omega Y_L(\Omega) Y_{L'}(\Omega) \\ &\times \exp \left\{ k \int_r^{r_{2,L}(\theta)} dr' K_{L'}(r', \theta) \right\} , \end{aligned} \quad (2.45)$$

where  $r_{2,L}(\theta)$  are the angle dependent external turning points, i.e. the largest root of the equation

$$\frac{V_0(r)}{E} - 1 + \frac{V_d(r, \theta)}{E} + \frac{(L + \frac{1}{2})^2}{k^2 r^2} = 0 , \quad (2.46)$$

at each angle. For LWKB approach, we can isolate the spherical contribution and write

$$\begin{aligned} \mathcal{H}_{L,L'}^{(LWKB)}(r) &= G_{L'}(r) \\ &\times \int d\Omega Y_L(\Omega) Y_{L'}(\Omega) \exp \left[ \frac{i}{\hbar} D_{0,L}(r, \theta) \right] \end{aligned} \quad (2.47)$$

where, according to Eq. (2.27)

$$D_{0,L}(r, \theta) \equiv -\frac{k}{2} \int_r^{r_{2,L}} dr' \frac{\Delta K(r', \theta)}{K_{0,L}(r')} , \quad (2.48)$$

is the deformed part of the exponential dependence generating the fundamental matrix of solutions. Here,  $G_L(r)$  is the solution of the spherical problem and given by (see appendix)

$$G_L(r) = \frac{1}{\sqrt{K_{0,L}(r)}} \exp \left[ \int_r^{r_{2,L}} dr' K_{0,L}(r') \right] , \quad (2.49)$$

and  $r_{2,L}$  is the *spherical* external turning point, i.e. the largest solution of the equation

$$\frac{V_0(r)}{E} - 1 + \frac{(L + \frac{1}{2})^2}{k^2 r^2} = 0 . \quad (2.50)$$

We note here that a somewhat similar treatment has been made by Stewart et al in [5] although the centrifugal

potential is introduced *ad hoc*, unlike in the AWKB approach of our paper. We also mention that in [6] the angular momentum dependence of the deformed correction is more approximate, while here we account for it completely. More precisely, the exponent in the deformed correction of Fröman's original work contains the ratio  $\Delta K/K_0(r)$ , but our LWKB treatment gives the rigorous angular momentum dependence of the deformed term.

A close inspection reveals that the LWKB deformed term in the fundamental matrix Eq. (2.47) can be regarded as a matrix which becomes unity in the case of 0 deformation. In order to compare the two approximations (with each other and with the CC equivalent), we have to force the spherical part in the AWKB method. This is done by defining

$$\mathcal{G}_{L,L'}(r) \equiv G_L(r)\delta_{L,L'} , \quad (2.51)$$

where  $G_L$  are the solutions of the spherical problem (2.2). With this definition we can impose (in matrix form)

$$\mathcal{H}^{(\text{AWKB})} \equiv \mathcal{G}\Delta\mathcal{H}^{(\text{AWKB})} , \quad (2.52)$$

from which we get the deformed term  $\Delta\mathcal{H}$  as

$$\Delta\mathcal{H}_{L,L'}^{(\text{AWKB})} = \frac{1}{G_L}\mathcal{H}_{L,L'}^{(\text{AWKB})} . \quad (2.53)$$

A similar expansion can be performed for the CC fundamental matrix, but with  $G_L^{(\text{CC})}$  and  $\mathcal{H}^{(\text{CC})}$ , the *exact* spherical wave function for channel  $L$  and the *exact* deformed fundamental matrix respectively

$$\Delta\mathcal{H}_{L,L'}^{(\text{CC})} = \frac{1}{G_L^{(\text{CC})}}\mathcal{H}_{L,L'}^{(\text{CC})} . \quad (2.54)$$

For LWKB method, where the spherical term is already separated, we have

$$\Delta\mathcal{H}_{L,L'}^{(\text{LWKB})} = \int d\Omega Y_L(\Omega)Y_{L'}(\Omega) \exp\left[\frac{i}{\hbar}D_{0,L}(r,\theta)\right] . \quad (2.55)$$

Notice that the propagator matrix (2.39) in all cases is given by the obvious relation

$$\mathcal{K}_{LL'} = \Delta\mathcal{H}_{LL'}^{-1} . \quad (2.56)$$

We could also perform a more symmetric decomposition of the AWKB and CC fundamental matrices by defining the matrix (we drop the AWKB and CC indexes in the reminder of this section)

$$\bar{\mathcal{G}}_{L,L'}(r) = \begin{pmatrix} \sqrt{G_0(r)} & 0 & 0 & \dots \\ 0 & \sqrt{G_2(r)} & 0 & \dots \\ \dots & \dots & \dots & \dots \end{pmatrix} , \quad (2.57)$$

with which the deformed fundamental matrices can be written as

$$\mathcal{H} = \bar{\mathcal{G}}\Delta\bar{\mathcal{H}}\bar{\mathcal{G}} . \quad (2.58)$$

We invert the above equation and perform the sums in the matrix multiplication to obtain the analogs of Eqs. (2.53,2.54) in the form

$$\Delta\bar{\mathcal{H}}_{L,L'} = \frac{1}{\sqrt{G_L G_{L'}}}\mathcal{H}_{L,L'} . \quad (2.59)$$

### III. NUMERICAL RESULTS

In this section we compare the two approximations with the exact solution given by the CC method. We also perform a systematic analysis of alpha decays from even-even emitters within the deformed WKB approach.

#### A. Coupled channels approach versus WKB

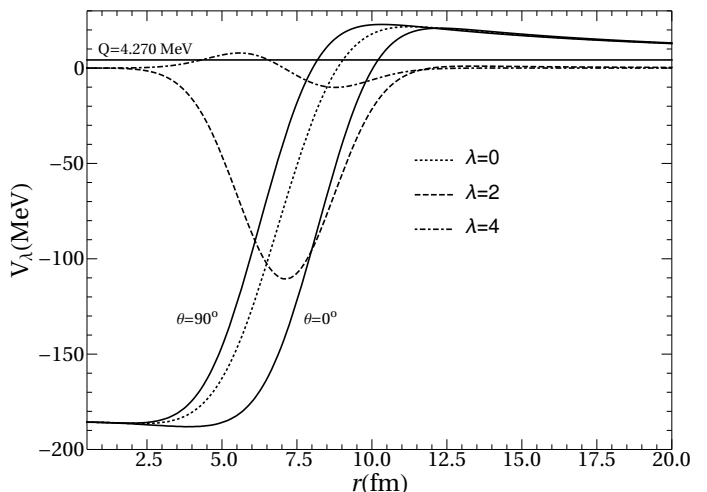


FIG. 2. Realistic alpha-daughter double-folding potential versus radius for the system  $^{234}\text{Th} + \alpha$ , plotted by a solid line for  $\theta = 0^\circ$  and  $\theta = 90^\circ$ . The multipoles are given by dotted ( $\lambda=0$ ), dashed ( $\lambda=2$ ) and dot-dashed lines ( $\lambda=4$ ). The horizontal line corresponds to the  $Q$ -value of the emission process  $^{238}\text{U} \rightarrow ^{234}\text{Th} + \alpha$   $Q=E=4.270$  MeV.

The realistic cluster-core interaction, given by the double-folding procedure [7–9], is plotted in Fig. 2 versus radius for the binary deformed system  $^{234}\text{Th} + \alpha$  with a quadrupole deformation  $\beta_2=0.215$ . The two solid curves correspond to  $\theta = 0^\circ$  and  $\theta = 90^\circ$ , respectively. The multipoles in Eq. (2.14) are given by dotted ( $\lambda=0$ ), dashed ( $\lambda=2$ ) and dot-dashed lines ( $\lambda=4$ ).

First we compare the amplitudes at the matching radius following the recipe in [5] for the  $^{238}\text{U}$  nucleus with scattering amplitudes (normalized to unity)  $\mathcal{N} = \{\sqrt{0.74}, \sqrt{0.25}, \sqrt{0.0004}\}$ . By using the expression of the total decay width [1]

$$\Gamma = \sum_{L=\text{even}} \Gamma_L = \hbar v \sum_{L=\text{even}} |N_L|^2 , \quad (3.1)$$

and (3.2) one can estimate the wave-function amplitudes at any point  $r$

$$f_L(r) = \sum_{L'} \mathcal{H}_{LL'}(r) \sqrt{\frac{\Gamma_{L'}}{\hbar v}}. \quad (3.2)$$

and must be normalized to unity as

$$f_L(r) \rightarrow \frac{f_L(r)}{\sum_{L'} |f_{L'}(r)|^2}. \quad (3.3)$$

We present the resulting amplitudes at  $R_m = 12.1$  fm in Table I showing remarkably close results considering that Stewart et al computed these amplitudes at the internal turning point.

TABLE I.  $R_m = 12.1$ fm

$L$	Stewart <i>et al</i>	LWKB	AWKB
0	+0.83	+0.83	+0.85
2	-0.55	-0.54	-0.52
4	-0.08	-0.15	-0.08

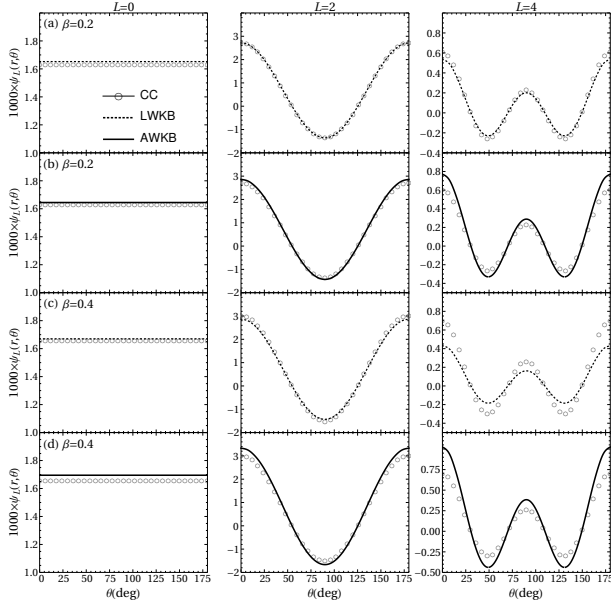


FIG. 3. The  $L = 0, 2, 4$  wave function components for CC (open symbols), LWKB (dots) and AWKB (solid line) for  $\beta_2 = 0.2$  (a) and (b) and  $\beta_2 = 0.4$  (c) and (d), estimated by using the fundamental matrix  $\mathcal{H}$ .

We have analyzed the accuracy of LWKB and AWKB approximations with respect to CC values. The results are given in Fig 3, where we plotted the CC wave function components for  $L = 0, 2, 4$  with open symbols for  $\beta_2 = 0.2$  (a), (b) and  $\beta_2 = 0.4$  (c), (d) at the barrier radius. By dots we plotted LWKB components and by solid lines AWKB components.

The results concerning the overall accuracy are shown in the Fig. 4. As  $\beta_2$  increases, we see that LWKB approximation gives a reasonable relative error

$$\sigma_X(r) = \sqrt{\frac{\sum_{LL'} [\mathcal{H}_{LL'}^{(X)}(r) - \mathcal{H}_{LL'}^{(CC)}(r)]^2}{\sum_{LL'} [\mathcal{H}_{LL'}^{(CC)}(r)]^2}}, \quad (3.4)$$

$X = LWKB, AWKB,$

about  $\sigma_{LWKB}(r_B) \sim 3\%$  for  $\beta_2 = 0.4$  at the barrier radius, while AWKB corresponds to a twice larger, but still relative small, value  $\sigma_{AWKB}(r_B) \sim 6\%$ .

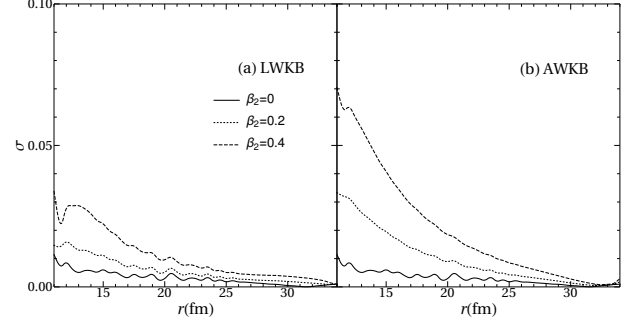


FIG. 4. (a) The relative error versus radius of the LWKB fundamental system of solutions versus its coupled channels counterpart. (b) Same as in (a) but for AWKB approach.

## B. Approximated interaction potential

The region between the internal turning point and the barrier maximum can be approximated with a good accuracy by an inverted parabola

$$V(r) - E = (V_B - E) \left[ 1 - \left( \frac{r_B - r}{r_B - r_1} \right)^2 \right] \equiv V_{frag} (1 - x^2), \quad (3.5)$$

in terms of the fragmentation potential

$$V_{frag} = V_B - E, \quad (3.6)$$

and dimensionless coordinate

$$x = \frac{r_B - r}{r_B - r_1}, \quad (3.7)$$

where  $r_1$  denotes the internal turning radius. The harmonic oscillator (ho) frequency parameter of the inverted parabola is given by

$$\hbar\omega = \frac{1}{r_B - r_1} \sqrt{\frac{V_{frag}}{d_\alpha}}, \quad (3.8)$$

in terms of the kinetic alpha-particle parameter

$$d_\alpha = \frac{2\mu_\alpha}{\hbar^2} \approx 0.192 \text{ MeV}^{-1} \text{ fm}^{-2}. \quad (3.9)$$

Our previous analysis has shown that  $\hbar\omega \sim 9$  MeV [10]. The internal potential is matched to the external Coulomb potential  $V_C(r) = 2Z_D/r$  at the barrier maximum  $r_B$ , because the difference with respect to the exact value is very small  $V_B = 0.94 V_C(r_B)$ .

The scattering amplitude is given at the barrier radius by using (2.38)

$$N_L = \frac{1}{G_L(\chi, \rho_B)} \sum_{L'} \mathcal{K}_{LL'}(r_B) f_{L'}^{(int)}(r_B), \quad (3.10)$$

where the WKB estimate of the internal wave-function is given at the barrier radius  $r_B$  by the Heel-Wheller ansatz [10]

$$f_L^{(int)}(V_{frag}) = \frac{\sqrt{p_L}}{C_{N,L}} \left( \frac{E}{V_{frag}} \right)^{\frac{1}{4}} \exp(-S_N^{(0)}), \quad (3.11)$$

in terms of the spherical nuclear action

$$S_N^{(0)} = \frac{\pi V_{frag}}{2\hbar\omega}, \quad (3.12)$$

and nuclear centrifugal term, given by the binomial approximation as follows

$$\begin{aligned} C_{N,L} &= \exp \left[ \left( L + \frac{1}{2} \right)^2 d \right] \\ d &= \frac{\delta}{2k} \sqrt{\frac{E}{V_{frag}}} \left[ \frac{\delta}{\Delta^2 r_B} + \frac{r_B}{\Delta^3} \left( \arctan \frac{\delta}{\Delta} - \frac{\pi}{2} \right) \right] \\ \delta &= r_B - r_1, \quad \Delta = \sqrt{r_B^2 - \delta^2}. \end{aligned} \quad (3.13)$$

The factor  $p_L$  is called alpha-formation probability, which can be determined by experimental channel widths.

Let us point out that we can use the potential, defined by (3.5), not only for the spherical part, but also for a deformed potential with  $V_B = V_B(\theta)$  being the maximum barrier height along the angle  $\theta$ ,  $r_B = r_B(\theta)$  its position and  $r_1 = r_1(\theta)$  the internal turning radius, which linearly depend upon the quadrupole deformation

$$r_a(\theta) = r_{a,0} [1 + b_a \beta_2 Y_{2,0}(\theta)], \quad a = B, 1.$$

By using this ansatz we can easily estimate the deformed part if the internal action  $D_N(\theta)$  defined by Eq. (2.48).

The WKB estimate of the Coulomb spherical multipole in (3.10) is given by

$$G_L(\chi, \rho) = C_{C,L} (\cot \alpha)^{\frac{1}{2}} \exp(S_C^{(0)}), \quad (3.14)$$

in terms of the spherical Coulomb action

$$S_C^{(0)} = \chi \left( \alpha - \frac{1}{2} \sin 2\alpha \right), \quad (3.15)$$

and Coulomb angular momentum term, given in a standard way by the binomial approximation

$$\begin{aligned} C_{C,L} &= \exp \left[ \left( L + \frac{1}{2} \right)^2 c \right] \\ c &= \frac{\tan \alpha}{\chi}. \end{aligned} \quad (3.16)$$

Here, we introduced the following parameter

$$\cos^2 \alpha = \frac{\rho}{\chi} = \frac{E}{V_C(r)}. \quad (3.17)$$

Notice that the above semiclassical estimate, valid for a pure Coulomb potential, gives 3% accuracy with respect to the exact function around the barrier region.

In order to estimate the fundamental and propagator matrix we used the separable LWKB approach (2.55). A simplified form is given by the Fröman approach (FWKB) [6], which neglects the centrifugal barrier in (2.48) and uses a sharp density distribution at the nuclear surface  $R = R_0 [1 + \beta_2 Y_{20}(\theta)]$ . The result is proportional to the quadrupole deformation parameter and Legendre polynomial

$$\begin{aligned} \frac{i}{\hbar} D_C^{(FWKB)}(\theta) &= -\beta_2 B(\chi, \rho) P_2(\cos \theta) \\ B(\chi, \rho) &\equiv \frac{\chi}{\sqrt{20\pi}} \sin 2\alpha (1 + \sin^2 \alpha). \end{aligned} \quad (3.18)$$

Thus, the deformed part of the fundamental matrix (2.55) within Fröman approach is given by

$$\begin{aligned} \Delta \mathcal{H}_{LL'}^{(FWKB)}(\beta_2, \chi, \rho) &= \int_{-1}^1 d \cos \theta \bar{P}_L(\cos \theta) \bar{P}_{L'}(\cos \theta) \\ &\quad \times \exp[-\beta_2 B(\chi, \rho) P_2(\cos \theta)], \end{aligned} \quad (3.19)$$

in terms of normalized Legendre polynomials

$$\bar{P}_L(\cos \theta) = \sqrt{\frac{2}{2L+1}} P_L(\cos \theta). \quad (3.20)$$

Therefore the Fröman propagator matrix (2.56) is given by

$$\begin{aligned} \mathcal{K}_{LL'}(\beta_2, \chi, \rho) &= \left[ \Delta \mathcal{H}_{LL'}^{(FWKB)}(\beta_2, \chi, \rho) \right]^{-1} \\ &= \Delta \mathcal{H}_{LL'}^{(FWKB)}(-\beta_2, \chi, \rho). \end{aligned} \quad (3.21)$$

### C. Alpha decay systematics

We analyzed available experimental decay widths concerning alpha-transitions from 168 the ground state of even-even emitters with  $J_i = 0$  to final states with  $J_f = L = 0, 2, 4, \dots$ . In Fig. 5 (a) are given the values of the reduced radius versus the Coulomb parameter at the barrier radius  $r_B = 1.429(A^{1/3} + 4^{1/3})$  by using transitions between ground states [10]. In the panel (b)



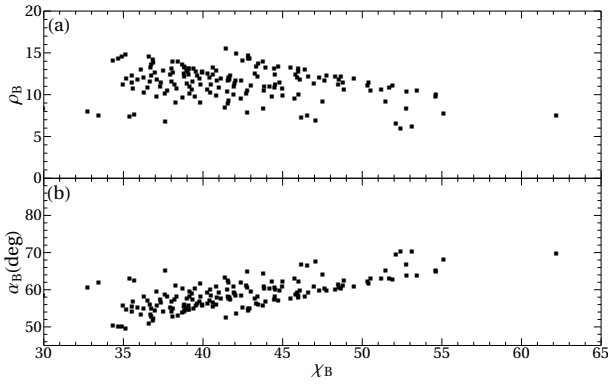


FIG. 5. (a) Reduced radius  $\rho_B$  as a function the Coulomb parameter at the barrier radius for alpha-transitions between ground states on even-even nuclei [10]. (b) Same as in (a), but for the angle  $\alpha_B$ .

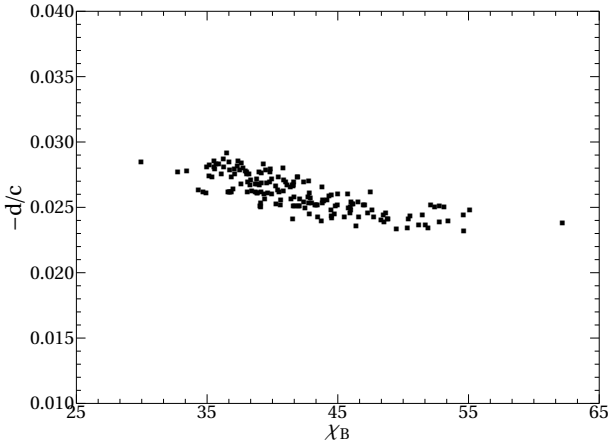


FIG. 6. Ratio between centrifugal terms  $-d/c$  versus Coulomb parameter.

we plotted the corresponding angle  $\alpha_B$  defined by Eq. (3.17). They span the following intervals (except one isolated point)

$$\begin{aligned} \chi_B &\in [33, 55] \\ \rho_B &\in [5, 15] \\ \alpha_B &\in [50^\circ, 70^\circ]. \end{aligned} \quad (3.22)$$

The last interval corresponds to a ratio between  $Q$ -value and the height of the Coulomb barrier

$$\frac{E}{V_B} \in [0.1, 0.4], \quad (3.23)$$

proving that the WKB approximation is very good for this kind of emission processes.

We analyzed the contribution of nuclear (3.13) and Coulomb centrifugal factors (3.16). From Fig. 6 we notice that the nuclear term is much smaller than its Coulomb counterpart

$$-d/c \in [0.025, 0.030], \quad (3.24)$$

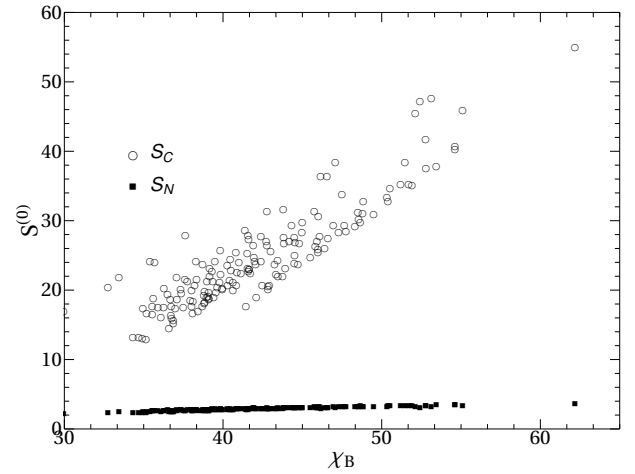


FIG. 7. Coulomb action  $S_C^{(0)}$  (open symbols) nuclear action  $S_N^{(0)}$  (dark symbols) versus Coulomb parameter for alpha-transitions between ground states of even-even nuclei.

and therefore it can be neglected.

We then compared the Coulomb to the internal nuclear action terms. First of all we notice from Fig. 7 that the spherical Coulomb term, plotted by open symbols, is much larger than the nuclear one, given by dark symbols

$$S_N^{(0)} \sim 2 \ll S_C^{(0)} \in [12, 50]. \quad (3.25)$$

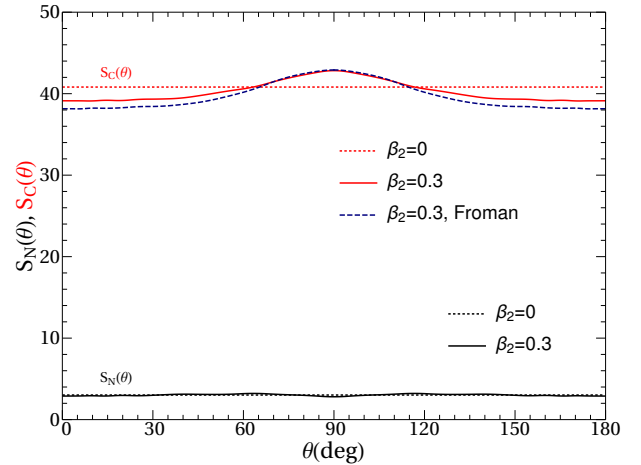


FIG. 8. Nuclear action (3.26) versus  $\theta$  within LWKB approach at the barrier radius  $r_B$  for  $\beta_2 = 0$  (dots) and for  $\beta_2 = 0.3$  (solid line). The corresponding upper lines correspond to the Coulomb action (3.27) within LWKB approach.

Thus, in Fig. 8 the lower plot gives the nuclear action

$$S_N(\theta) = S_N^{(0)} + D_N(\theta), \quad (3.26)$$

within LWKB approach at the barrier radius  $r_B$  for  $\beta_2 = 0$  by dots and for  $\beta_2 = 0.3$  by a solid line. The corresponding upper lines correspond to the Coulomb action

within LWKB approach.

$$S_C(\theta) = S_C^{(0)} + D_C(\theta), \quad (3.27)$$

Notice that the Fröman FWKB estimate for the Coulomb action (3.18), plotted by a dashed line, gives close values.

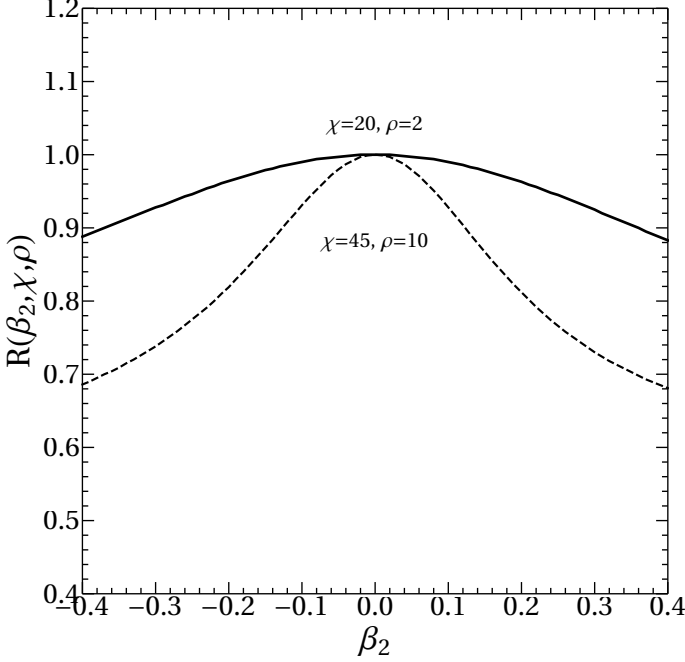


FIG. 9. Ratio between diagonal and all propagator matrix elements  $R(\beta_2, \chi, \rho)$  (3.43) versus quadrupole deformation for an alpha decay with average parameters  $\chi = 45$ ,  $\rho = 10$  (lower dashed line) and proton emission with  $\chi = 20$ ,  $\rho = 2$  (upper solid line).

Therefore it turns out that the angular dependence is practically given by the Coulomb terms, due to the fact the nuclear part is practically constant in this scale  $S_N(\theta) \sim S_N^{(0)}(\theta)$ . Thus, the largest internal function computing scattering amplitudes in Eq. (3.10) is practically monopolar  $|f_0^{(int)}| \gg |f_L^{(int)}|$ ,  $L = 2, 4, \dots$  and therefore one obtains the following estimate

$$N_L \approx \frac{f_0^{(int)}(V_{frag})}{G_L(\chi_B, \rho_B)} \mathcal{K}_{L0}(\beta_2, \chi_B, \rho_B). \quad (3.28)$$

Indeed, by using Eq. (3.2) with realistic channel decay widths, it turns out that  $|f_L^{(int)}| < 10^{-3}|f_0^{(int)}|$ ,  $L = 2, 4, 6$ . Until now we analyzed transitions between ground states. Deformation effects are probed by the analysis of the fine-structure revealed by transitions to excited states in the daughter nucleus. We neglected in our formalism the contribution of the daughter dynamics. The emitted alpha-particle with angular momentum  $L$  is coupled with the same angular momentum of the daughter nucleus to the initial spin  $J_i = 0$ . Thus, in each channel the energy is replaced by  $E \rightarrow E - E_L$ , where  $E_L$  is

the excitation energy of the daughter nucleus [1]. As we already mentioned, by neglecting non-diagonal Coriolis matrix elements in the intrinsic system of coordinates, the decoupled system of equations at large distances (2.4) becomes formally the same [1, 6], but the Coulomb parameter and reduced radius for each channel are given by Eqs. (2.15). At the barrier radius these relations become

$$\begin{aligned} \chi_L &= \frac{\chi_B}{\epsilon_L} \\ \rho_L &= \rho_B \epsilon_L \\ \epsilon_L &\equiv \sqrt{1 - \frac{E_L}{E}}, \end{aligned} \quad (3.29)$$

where the values  $\chi_B$ ,  $\rho_B$  are the barrier values for  $L = 0$ . Thus, the total decay width (3.1) becomes a superposition of channel decay widths as follows

$$\Gamma = \sum_{L=even} \Gamma_L = \sum_{L=even} \hbar v_L |N_L|^2, \quad (3.30)$$

in terms of the channel velocity

$$v_L = \sqrt{\frac{2E}{\mu}} \epsilon_L, \quad (3.31)$$

where the scattering amplitude (3.28) is replaced by

$$N_L = \frac{f_0^{(int)}(V_{frag}^L)}{G_L(\chi_L, \rho_L)} \mathcal{K}_{L0}(\beta_2, \chi_B, \rho_B). \quad (3.32)$$

Thus, each channel decay width (3.30) for transitions from the ground state with  $J_i = 0$  to final states with  $J_f = L$  becomes factorized

$$\Gamma_L = \Gamma_L^{(0)}(\chi_L, \rho_L) D_L(\beta_2, \chi_L, \rho_L), \quad (3.33)$$

into a spherical "monopole"

$$\begin{aligned} \Gamma_L^{(0)}(\chi_L, \rho_L) &= \hbar v_L \left[ \frac{f_0^{(int)}(V_{frag}^L)}{G_0(\chi_L, \rho_L)} \right]^2 \\ &= \hbar v_L p_0 \exp \left[ -2 \left( S_C^{(0)}(\chi_L, \rho_L) + S_N^{(0)}(V_{frag}^L) \right) \right], \end{aligned} \quad (3.34)$$

in terms of the channel fragmentation potential

$$V_{frag}^L = V_B - (E - E_L) = V_{frag} + E_L, \quad (3.35)$$

and centrifugal-deformation factor

$$\begin{aligned} D_L(\beta_2, \chi_L, \rho_L) &= \exp \left[ -2 \frac{\tan \alpha_L}{\chi_L} L(L+1) \right] \\ &\times \mathcal{K}_{L0}^2(\beta_2, \chi_B, \rho_B), \end{aligned} \quad (3.36)$$

induced by the deformed Coulomb field. Here we used the exact quantum expression  $L(L+1)$  due to the fact that the alpha-decay fine structure involves low values of the angular momentum.

One can also factorize the "monopole" decay width

$$\Gamma_L^{(0)}(\chi_L, \rho_L) = \gamma_0^2 (V_{frag}^L) P_0(\chi_L, \rho_L), \quad (3.37)$$

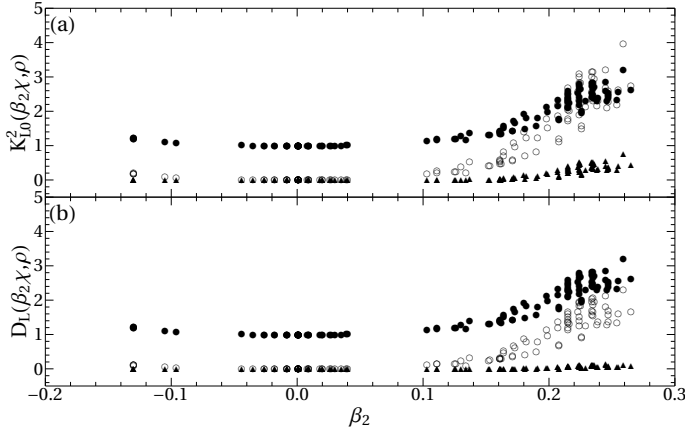


FIG. 10. (a) The deformation factor  $\mathcal{K}_{L0}^2(\beta_2, \chi_B, \rho_B)$  versus deformation for  $L = 0$  (dark circles),  $L = 2$  (open circles) and  $L = 4$  (triangles). (b) Same as in (a), but for the centrifugal-deformation factor  $D_L(\beta_2, \chi, \rho)$  (3.36).

in terms of the channel reduced width and penetrability

$$\begin{aligned} \gamma_0^2(V_{frag}^L) &= p_0 \exp \left[ -2S_N^{(0)}(V_{frag}^L) \right] \\ P_0(\chi_L, \rho_L) &= \hbar v_L \exp \left[ -2S_C^{(0)}(\chi_L, \rho_L) \right], \end{aligned} \quad (3.38)$$

and therefore the channel decay width can be factorized

$$\Gamma_L = \gamma_0^2(V_{frag}^L) P_L(\beta_2, \chi_L, \rho_L), \quad (3.39)$$

in terms of the channel reduced width and deformed penetrability

$$P_L(\beta_2, \chi_L, \rho_L) = P_0(\chi_L, \rho_L) D_L(\beta_2, \chi_L, \rho_L). \quad (3.40)$$

Our estimate has shown that the following approximation

$$D_L(\beta_2, \chi_L, \rho_L) \approx D_L(\beta_2, \chi_B, \rho_B), \quad (3.41)$$

remains valid within 5% accuracy at  $\beta_2 = 0.3$  and it can be used in the above relation. This approximate ansatz for FWKB was used in the Fröman paper [6], but here it was neglected the channel dependence of the Coulomb action and the nuclear part was not considered. Anyway, it turns out that the main channel energy dependence connected to the daughter dynamics is exponentially induced by Coulomb and nuclear action terms in Eq. (3.34).

Now we can explain the alignment of open symbols in Fig. 7 along parallel straight lines. This feature corresponds to the well known Geiger-Nuttall law for alpha transitions between ground states

$$\begin{aligned} \log_{10} T_0 &\sim \log_{10} \left[ \frac{G_0(r_B)}{f_0^{(int)}(r_B)} \right]^2 \sim 2 \left[ S_C^{(0)} + S_N^{(0)} \right] \\ &= 2\chi \left( \alpha - \frac{1}{2} \sin 2\alpha \right) + \frac{\pi V_{frag}}{\hbar\omega} \\ &\sim a \frac{Z}{\sqrt{E}} + b, \end{aligned} \quad (3.42)$$

where  $a$  and  $b$  are constants.

Let us stress on the fact that the factorized representation (3.33) with (3.34) and (3.36) remains valid for any of the above described approximations AWKB, LWKB and FWKB. Moreover, we have shown in Fig. 8 that LWKB results are close to the Fröman FWKB approach. In order to point out on the deformation effect of the propagator matrix we plotted in Fig. 9 by the lower dashed line the following ratio

$$R(\beta_2, \chi, \rho) = \frac{S_{diag}}{S_{total}} = \sqrt{\frac{\sum_L \mathcal{K}_{LL}^2(\beta_2, \chi, \rho)}{\sum_{L,L'} \mathcal{K}_{L'L'}^2(\beta_2, \chi, \rho)}}, \quad (3.43)$$

for  $\chi = 45$ ,  $\rho = 10$  by using FWKB. This quantity gives an overall characteristics on the coupling between channels induced by the quadrupole deformation. One sees that the overall deformation effects are rather strong, i.e.  $R \sim 0.73$  at  $\beta_2 \sim 0.3$ . As a comparison, we plotted by the upper solid line the same ratio for proton emission corresponding to characteristic parameters  $\chi = 20$ ,  $\rho = 2$ . Notice a significantly smaller effect  $R \sim 0.93$  at the same deformation. One can conclude that the deformation effect is mainly enhanced by the increase of the Coulomb parameter  $\chi$ .

We then analyzed the influence of the deformation on each channel decay width by plotting in Fig. 10 (a) the deformation factor, i.e. the propagator matrix element squared  $\mathcal{K}_{L0}^2(\beta_2, \chi_B, \rho_B)$  multiplying the spherical decay width, versus deformation for  $L = 0$  (dark circles),  $L = 2$  (open circles) and  $L = 4$  (triangles). One clearly sees that the deformation effect induced by the Coulomb barrier plays a significant role on each partial decay width for  $\beta_2 > 0.1$ , especially for the quadrupole  $L = 2$ , but also for the monopole  $L = 0$  channel. In the panel (b) we plotted the centrifugal-deformation factor (3.36) versus deformation. One clearly sees that the  $L = 0, 2$  channels are the most relevant in the structure of the channel decay width.

The logarithm of the theoretical channel hindrance factor, estimated by using the explicit form of the internal wave function predicts the following dependence

$$\begin{aligned} \log_{10} HF_L &= \log_{10} \frac{\gamma_0^2(V_{frag})}{\gamma_0^2(V_{frag}^L)} \\ &\sim \log_{10} \frac{p_0}{p_L} + 2 \left[ S_N(V_{frag}^L) - S_N(V_{frag}) \right] \log_{10} e \\ &\sim (\log_{10} p_0 - \log_{10} p_L) + E_L. \end{aligned} \quad (3.44)$$

We investigate the experimental hindrance factor

$$HF_L(exp) = \frac{\gamma_0^2(exp)}{\gamma_L^2(exp)}, \quad (3.45)$$

defined in terms of the experimental reduced width

$$\gamma_L^2(exp) = \frac{\Gamma_L(exp)}{P_L(\beta_2, \chi_L, \rho_L)}. \quad (3.46)$$

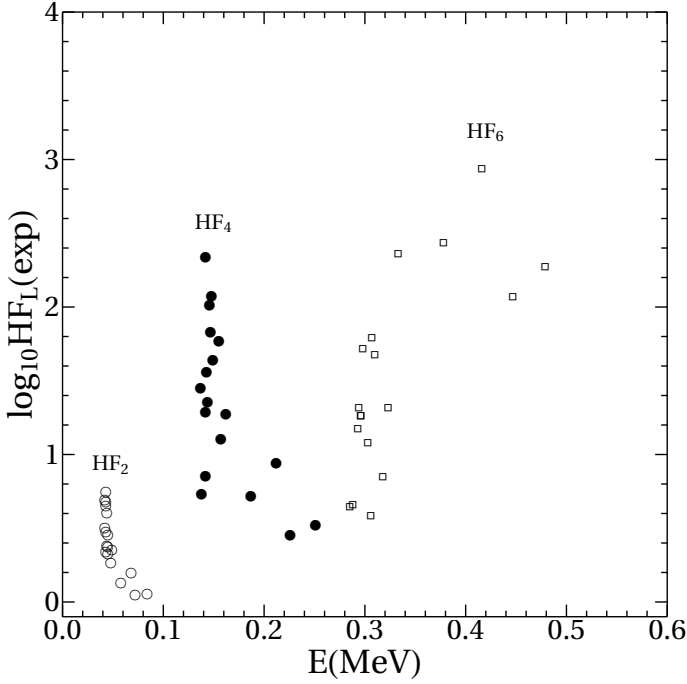


FIG. 11. Experimental hindrance factor (3.45) versus the excitation energy of the daughter nucleus for  $L = 2$ , (open circles)  $L = 4$  (dark circles) and  $L = 6$  (open squares).

In Fig. 11 we plotted  $HF_L(exp)$  versus the excitation energy of the daughter nucleus  $E_L$ , for  $L = 2$ , (open circles)  $L = 4$  (dark circles) and  $L = 6$  (open squares) corresponding to 18 well deformed emitters above  $^{208}\text{Pb}$  with measured channel decay widths. One indeed sees that the general trend follows the linear energy dependence of Eq. (3.44). At the same time, notice the local strong decrease of each  $\log_{10} HF_2$  and  $\log_{10} HF_4$  along with the increase of the excitation energy. This feature is given by the strong increase of the channel probability  $p_L$  with respect to the excitation energy increase along each  $L$ -channel.

#### IV. CONCLUSIONS

We compared the exact coupled channels procedure to the semiclassical approach to describe two-body emission processes from deformed nuclei by using the propagator method. We expressed within this approach the vector of scattering amplitudes in terms of a propagator matrix multiplied by the vector of internal radial wave function components divided to the vector of irregular Coulomb waves. We described in a rigorous way the 3D semiclassical approach, corresponding to deformed potentials, which leads to the exact results for the propagator matrix. We compared them with the much simpler expressions given by the AWKB and LWKB with its approximation, known as Fröman method. We have

shown that LWKB approach is closer than AWKB to the exact coupled-channels formalism. Each channel decay width becomes factorized into spherical and centrifugal-deformed terms. An analysis of deformation effects for alpha-emission from ground states of even-even nuclei was performed. We evidenced the important role played by deformation.

#### ACKNOWLEDGMENTS

This work was supported by the grant of the Romanian Ministry Education and of Research PN-18090101/2019-2021 and by the grant of the Institute of Atomic Physics from the National Research – Development and Innovation Plan III for 2015 -2020/Programme 5/Subprograme 5.1 ELI-RO, project ELI-RO No 12/2020.

#### Appendix: WKB wave function and quantization in 3D

What we present in this appendix is not new by any means, but to the best of our knowledge, there is no comprehensive work clearly stating all considerations involved in finding a proper solution for the spherical WKB system from Eqs. (2.9). We start by re-writing system (2.9)

$$\begin{aligned} \hbar^0 : (\nabla S_0^{(0)}(\mathbf{r}))^2 &= -K_0^2(r) \\ \hbar^1 : -\frac{i}{2} \Delta S_0^{(0)}(\mathbf{r}) + (\nabla S_0^{(0)}(\mathbf{r}))(\nabla S_0^{(1)}(\mathbf{r})) &= 0 \end{aligned} \quad (\text{A.1})$$

The equation for the first order in  $\hbar$  can be solved by means of separation of variables. We, thus, write

$$S_0^{(0)}(\mathbf{r}) = A^{(0)}(r) + B^{(0)}(\theta) + C^{(0)}(\phi)$$

and obtain

$$\begin{aligned} [\nabla S_0^{(0)}(\mathbf{r})]^2 &= \\ &= \left( \frac{dA^{(0)}(r)}{dr} \right)^2 + \left( \frac{1}{r} \frac{dB^{(0)}(\theta)}{d\theta} \right)^2 + \left( \frac{1}{r \sin \theta} \frac{dC^{(0)}(\phi)}{d\phi} \right)^2 \\ &= -2\mu (V_0(r) - E) \end{aligned} \quad (\text{A.2})$$

from here on we employ the notation

$$K_0(r) \equiv \sqrt{2\mu E \left[ \frac{V_0(r)}{E} - 1 \right]} \quad (\text{A.3})$$

We separate  $\phi$  in the above equation and solve for  $C(\phi)$

$$\begin{aligned} - \left( \frac{dC^{(0)}}{d\phi} \right)^2 &= -\lambda_\phi^2 \\ &= r^2 \sin^2 \theta \left[ \left( \frac{dA^{(0)}}{dr} \right)^2 + \frac{1}{r^2} \left( \frac{dB^{(0)}}{d\theta} \right)^2 + K_0^2 \right] \end{aligned} \quad (\text{A.4})$$

where  $\lambda_\phi$  is a separation constant, which will be determined through quantization. As expected, we obtain a periodic dependence on  $\phi$  in our wave function through

$$C^{(0)}(\phi) = \pm \lambda_\phi \phi \quad (\text{A.5})$$

We now separate  $\theta$

$$\begin{aligned} - \left( \frac{dB^{(0)}}{d\theta} \right)^2 - \frac{\lambda_\phi^2}{\sin^2 \theta} &= -\lambda_\theta^2 \\ &= r^2 \left[ \left( \frac{dA^{(0)}}{dr} \right)^2 + K_0^2 \right] \end{aligned} \quad (\text{A.6})$$

where  $\lambda_\theta$  is another separation constant. Rearranging the  $\theta$  part gives

$$\frac{dB^{(0)}}{d\theta} = \pm \sqrt{\lambda_\theta^2 - \frac{\lambda_\phi^2}{\sin^2 \theta}} \quad (\text{A.7})$$

The closed form of  $B(\theta)$  is not, at this point, of interest to us so we proceed with the last variable for which

$$\left( \frac{dA^{(0)}}{dr} \right)^2 = -K_0^2 - \frac{\lambda_\theta^2}{r^2} \quad (\text{A.8})$$

which, upon expanding all terms, takes the familiar form

$$\frac{dA^{(0)}}{dr} = \pm i \sqrt{2\mu E \left( \frac{V_0(r)}{E} - 1 + \frac{\lambda_\theta^2}{r^2} \right)} \quad (\text{A.9})$$

Now we could address the quantization procedure. The astute reader can already guess that if one stops here and performs the quantization only to the first order, the separation constants would become [11] (by straight forward identification)

$$\begin{aligned} \lambda_\phi &= M\hbar \\ \lambda_\theta &= \left( L + \frac{1}{2} \right) \hbar \end{aligned} \quad (\text{A.10})$$

where  $M$  is the magnetic quantum number and  $L$  is the usual orbital quantum number. A full account of the above expressions and the reason for the Langer correction ( $\sqrt{L(L+1)} \rightarrow L+1/2$ ) [12] will be given later on. However, to increase the accuracy of the WKB method we have to compute also the second order contribution which, rigorously speaking, must enter in the quantization procedure. We notice that the second equation in (A.1) is also separable given the expression we found for the first order contribution. We can thus write

$$S_0^{(1)}(\mathbf{r}) = A^{(1)}(r) + B^{(1)}(\theta) + C^{(1)}(\phi) \quad (\text{A.11})$$

which implies (by direct substitution)

$$\begin{aligned} &\frac{i}{2} \left( \frac{d^2 A^{(0)}}{dr^2} + \frac{2}{r} \frac{dA^{(0)}}{dr} + \frac{1}{r^2} \frac{d^2 B^{(0)}}{d\theta^2} + \frac{\cot \theta}{r^2} \frac{dB^{(0)}}{d\theta} \right) \\ &= \frac{dA^{(0)}}{dr} \frac{dA^{(1)}}{dr} + \frac{1}{r^2} \frac{dB^{(0)}}{d\theta} \frac{dB^{(1)}}{d\theta} + \frac{1}{r^2 \sin^2 \theta} \frac{dC^{(0)}}{d\phi} \frac{dC^{(1)}}{d\phi} \end{aligned} \quad (\text{A.12})$$

We separate first the  $\phi$  dependence and obtain

$$\begin{aligned} &\frac{ir^2 \sin^2 \theta}{2} \left( \frac{d^2 A^{(0)}}{dr^2} + \frac{2}{r} \frac{dA^{(0)}}{dr} + \frac{1}{r^2} \frac{d^2 B^{(0)}}{d\theta^2} + \frac{\cot \theta}{r^2} \frac{dB^{(0)}}{d\theta} \right) \\ &- r^2 \sin^2 \theta \left( \frac{dA^{(0)}}{dr} \frac{dA^{(1)}}{dr} + \frac{1}{r^2} \frac{dB^{(0)}}{d\theta} \frac{dB^{(1)}}{d\theta} \right) \\ &= \frac{dC^{(0)}}{d\phi} \frac{dC^{(1)}}{d\phi} = \gamma_\phi \end{aligned} \quad (\text{A.13})$$

where  $\gamma_\phi$  is another separation constant and, solving for  $C^{(1)}$  we find

$$C^{(1)}(\phi) = \pm \frac{\gamma_\phi}{\lambda_\phi} \phi. \quad (\text{A.14})$$

where  $\gamma_\phi$  is another separation constant. We address now the quantization of the  $\phi$  motion. The generally accepted semiclassical quantization is the Einstein-Brillouin-Keller (EBK) condition which reads [13]

$$\frac{1}{2\pi} \oint P_q dq = \left( n_q + \frac{\mu_i}{4} + \frac{b_i}{2} \right) \hbar \quad (\text{A.15})$$

where  $q$  is the generalized variable,  $P_q$  is its associated generalized momentum,  $n_q$  is the standard quantum number for that variable,  $\mu_q, b_q$  are Maslov indexes ( $\mu_q$  is the number of conventional turning points along the integration path and  $b_q$  is the number of hard-wall turning points along the integration path). The integration path is the path traversed by the classical particle in one complete period. In the case of the  $\phi$  motion, the integration path is  $[0, 2\pi]$  since this corresponds to a complete  $\phi$  period and the whole range is classically allowed. The generalized momentum is given by

$$P_\phi \equiv \frac{\partial S}{\partial \phi} = \left( \lambda_\phi + \hbar \frac{\gamma_\phi}{\lambda_\phi} \right) \quad (\text{A.16})$$

The quantization condition reads

$$\frac{1}{2\pi} \oint P_\phi d\phi = \frac{1}{2\pi} \int_0^{2\pi} d\phi \left( \lambda_\phi + \hbar \frac{\gamma_\phi}{\lambda_\phi} \right) = n_\phi \hbar \quad (\text{A.17})$$

since the integrand and we obtain

$$\lambda_\phi + \hbar \frac{\gamma_\phi}{\lambda_\phi} = n_\phi \hbar \quad (\text{A.18})$$

We now turn back to  $\theta$  and apply a similar reasoning as we did for  $\phi$

$$\begin{aligned} &\frac{dB^{(0)}}{d\theta} \frac{dB^{(0)}}{d\theta} + \frac{\gamma_\phi}{\sin^2 \theta} - \frac{i}{2} \frac{d^2 B^{(0)}}{d\theta^2} - \frac{i \cot \theta}{2} \frac{dB^{(0)}}{d\theta} \\ &= \frac{ir^2}{2} \left( \frac{d^2 A^{(0)}}{dr^2} + \frac{2}{r} \frac{dA^{(0)}}{dr} \right) \\ &= \gamma_\theta \end{aligned} \quad (\text{A.19})$$

where  $\gamma_\theta$  is another separation constant. After some rearrangements we can write

$$\frac{dB^{(1)}}{d\theta} = \frac{i}{2} \frac{1}{\frac{dB^{(0)}}{d\theta}} \frac{d^2 B^{(0)}}{d\theta^2} + \frac{i}{2} \cot \theta + \frac{1}{\frac{dB^{(0)}}{d\theta}} \left( \gamma_\theta - \frac{\gamma_\phi}{\sin^2 \theta} \right) \quad (\text{A.20})$$

with  $\gamma_\theta$  another separation constant. A discussion is called for here regarding the last two separation constants. With the constraints derived up to now, they could take any value subject, of course, to the quantization conditions. We saw that for the  $\phi$  dependence,  $\gamma_\phi$  does not make any difference aside from a phase. The problem, however arises for the  $\theta$  dependence. If we now try to make the analogy with the exact result, we see that  $\gamma_\phi$  and  $\gamma_\theta$  should be set to 0. Indeed starting from the system of equations for the Legendre associated functions  $P_{L,M}(\theta)$  and the azimuth function  $\Phi$

$$\begin{aligned} \frac{d^2 P_{L,M}}{d\theta^2} + \cot \theta \frac{dP_{L,M}}{d\theta} + \left( L(L+1) - \frac{M^2}{\sin^2 \theta} \right) P_{L,M} &= 0 \\ \frac{d^2 \Phi}{d\phi^2} &= -M^2 \Phi \end{aligned}$$

and perform the semiclassical expansion on both equations independently, we see that only 2 constants arise. This implies that  $\gamma_\phi = \gamma_\theta = 0$ .

In the light of the above considerations we can write

$$\frac{dB^{(1)}}{d\theta} = \frac{i}{2} \frac{1}{\frac{dB^{(0)}}{d\theta}} \frac{d^2 B^{(0)}}{d\theta^2} + \frac{i}{2} \cot \theta \quad (\text{A.21})$$

with the solution given by

$$B^{(1)}(\theta) = \frac{i}{2} \log \left| \frac{dB^{(0)}}{d\theta} \right| + \frac{i}{2} \log \sin(\theta) \quad (\text{A.22})$$

Now we have to determine  $\lambda_\theta$  which is done through the quantization condition

$$\frac{1}{2\pi} \oint P_\theta d\theta = \left( n_\theta + \frac{\mu_\theta}{4} + \frac{b_\theta}{2} \right) \hbar \quad (\text{A.23})$$

with

$$P_\theta \equiv \frac{dS_0}{d\theta} = \frac{dB^{(0)}}{d\theta} + \hbar \frac{dB^{(1)}}{d\theta} \quad (\text{A.24})$$

In this case, the classically allowed range for  $\theta$  is  $[\frac{\pi}{2} - \gamma, \frac{\pi}{2} + \gamma]$  where  $\gamma = \arccos(\lambda_\phi/\lambda_\theta)$ , meaning that the integration contour is 2 times this range. Moreover, there are two classical turning points at the end of the range with

no hard-walls, hence  $\mu_\theta = 2$  and  $b_\theta = 0$  so Eq. (A.23) becomes

$$\frac{1}{\pi} \int_{\frac{\pi}{2}-\gamma}^{\frac{\pi}{2}+\gamma} d\theta \sqrt{\lambda_\theta^2 - \frac{\lambda_\phi^2}{\sin^2 \theta}} \equiv I_\theta = \left( n_\theta + \frac{1}{2} \right) \hbar \quad (\text{A.25})$$

because the logarithms evaluated along this contour give no contribution (no poles inside the integration domain). To solve the integral above, we follow the approach in chapter 13 of [14], but we mention that the  $\theta$  allowed region is the one given above. First we change the variable using

$$\cos \theta = \sin \gamma \sin \eta$$

which gives after some rearrangements

$$I_\theta = \frac{\lambda_\theta}{\pi} \int_{-\frac{\pi}{2}}^{\frac{\pi}{2}} d\eta \frac{\sin^2 \gamma \cos^2 \eta}{1 - \sin^2 \gamma \sin^2 \eta}$$

then, with another change of variable

$$u = \tan \eta$$

the integral becomes

$$I_\theta = \frac{\lambda_\theta}{\pi} \int_{-\infty}^{\infty} du \frac{\sin^2 \gamma}{(1+u^2)(1+u^2 \cos^2 \gamma)} \quad (\text{A.26})$$

$$= \frac{\lambda_\theta}{\pi} \int_{-\infty}^{\infty} du \left( \frac{1}{1+u^2} - \frac{\cos^2 \gamma}{1+u^2 \cos^2 \gamma} \right) \quad (\text{A.27})$$

$$= \frac{\lambda_\theta}{\pi} (\arctan u - \cos \gamma \arctan(u \cos \gamma)) \Big|_{-\infty}^{\infty} \quad (\text{A.28})$$

$$= \lambda_\theta - \lambda_\phi \quad (\text{A.29})$$

Adding the result above to Eq. (A.18) and taking into account that  $\gamma_\phi = 0$  gives

$$\lambda_\theta = \left( n_\theta + n_\phi + \frac{1}{2} \right) \hbar \quad (\text{A.30})$$

which, if we denote  $L = n_\theta + n_\phi$ , can be written as

$$\lambda_\theta = L + \frac{1}{2} \quad (\text{A.31})$$

Now, we can solve for  $r$  and we find that

$$\frac{dA^{(1)}}{dr} = \frac{i}{2} \frac{1}{\frac{dA^{(0)}}{dr}} \frac{d^2 A^{(0)}}{dr^2} + ir$$

which gives

$$A^{(1)}(r) = \frac{i}{2} \log \left( \left| \frac{dA^{(0)}}{dr} \right| \right) + i \log(r) \quad (\text{A.32})$$

We now gather all results together and obtain the WKB approximation of the wave function for the 3D motion as a superposition of "incoming" and "outgoing" functions

$$\Psi_0(\mathbf{r}) = \frac{Y_{LM}^{(\text{WKB})}(\theta, \phi)}{\sqrt{K_{0,L}(r)}} \left\{ c_L^{(\text{out})} \exp \left[ \int_{r_0}^r dr' K_{0,L}(r') \right] + c_L^{(\text{in})} \exp \left[ - \int_{r_0}^r dr' K_{0,L}(r') \right] \right\}, \quad (\text{A.33})$$

where  $Y_{L,M}^{(\text{WKB})}$  is the WKB approximation of the spherical harmonic  $Y_{L,M}$  and  $r_0$  is the starting point of integration. We do not give the closed form of  $Y_{L,M}$  since it is more complicated and not useful as we can use the exact result. However, the reader is advised to consult ref. [15] for a complete account, or [16], for the case  $M = 0$ . We also mention here the works of Robnik [17, 18] who attempts a general quantization to all orders under some conjecture and the work of Salasnich [19]. Both authors show that under some special circumstances, the quan-

tum eigenvalue of the angular momentum operator can be retrieved from semiclassical calculations.

Finally, since it is helpful for the studies in this work, we give here the form of the radial part of an outgoing solution of the spherical problem

$$G_L(r) = \frac{1}{\sqrt{K_{0,L}(r)}} \exp \left[ \int_r^{r_{2,L}} dr' K_{0,L}(r') \right], \quad (\text{A.34})$$

where  $r_{2,L}$  is the external turning point.

- 
- [1] D.S. Delion, *Theory of Particle and Cluster Emission*, (Springer, 2010)
  - [2] G. Gamow, *Z. Phys.* **51**, 204 (1928).
  - [3] E.U. Condon and R.W. Gurney, *Nature* **122**, 439 (1928).
  - [4] Delion, D. S. and Liotta, R. J. and R. Wyss, *Phys. Rev. C* **92**, 051301 (2015).
  - [5] T.L. Stewart, M.W. Kermode, D.J. Beachey, N. Rowley, I.S. Grant, and A.T. Kruppa, *Phys. Rev. Lett.* **77**, 36 (1996).
  - [6] P.O. Fröman, *Mat. Fys. Scr. Dan. Vid. Selsk.* **1** no. 3 (1957).
  - [7] G. Bertsch, J. Borysowicz, H. McManus, and W.G. Love, *Nucl. Phys. A* **284**, 399 (1977).
  - [8] G.R. Satchler and W.G. Love, *Phys. Rep.* **55**, 183 (1979).
  - [9] F. Carstoiu and R.J. Lombard, *Ann Phys. (NY)*, **217**, 279 (1992).
  - [10] D.S. Delion and A. Dumitrescu, *Phys. Rev. C* **102**, 014327 (2020).
  - [11] L.J. Curtis and D.J. Ellis, *Amer. J. Phys.*, **72** (2004).
  - [12] R.E. Langer, *Phys. Rev.* **51**, 669 (1937).
  - [13] M. Brack and R. Bhaduri, *Semiclassical Physics* (Avalon Publishing, 2003).
  - [14] H. Goldstein, C.P. Poole, and J.L. Safko, *Classical Mechanics*, (Addison Wesley, 2002).
  - [15] R. More, *Journal de Physique II* **1**, 97 (1991).
  - [16] L.D. Landau and E.M. Lifshitz *Quantum Mechanics (Third Edition)* (Pergamon, 1977).
  - [17] M. Robnik and L. Salasnich, *J. Phys. A* **30**, 1719 (1997).
  - [18] M. Robnik and L. Salasnich, *J. Phys. A* **30**, 1711 (1997).
  - [19] L. Salasnich and F. Sattin, *J. Phys. A* **30**, 7597 (1997).